Appl. Phys. B 58, 397–402 (1994)

Applied Physics B Lasers and Optics

Temperature Dependence of Efficiency and Thermal Lensing of Diode-Laser-Pumped Nd:YAG Lasers

U. Brauch

Institut für Technische Physik, Deutsche Forschungsanstalt für Luft- und Raumfahrt e. V., Pfaffenwaldring 38-40, D-70569 Stuttgart, Germany (Tel.: 49-711/6862-512, Fax: 49-711/6862-715)

Received 8 October 1993/Accepted 13 January 1994

Abstract. Efficiencies, lasing thresholds and thermal lensing of a Nd:YAG rod side-pumped with two 10 W diode-laser-arrays are measured for various rod temperatures between 80 K and 380 K. The threshold is reduced by a factor of 2.5–4 on cooling from room temperature to about 100 K, while the slope efficiency is increased by between 0% and 50% depending on the reflectivity of the outcoupling mirror. Extrapolation to a 240 W pumped laser gives an increase in optical efficiency of 25% to 30%. The thermal lensing measured with a beam deflection and an interferometric method is reduced by a factor of 10.

PACS: 42.55.Rz

Experiments with solar-pumped Nd:YAG and Nd:GSGG lasers have shown that operation under high thermal load at 80 K (liquid-nitrogen cooling) is more efficient than at room temperature (water cooling) [1]. Even though the absorption efficiency of the blackbody-like solar spectrum is much lower because of the line narrowing, this is overcompensated by the high gain and the strongly improved thermal properties (thermal lensing and thermally induced birefringence).

Use of narrow-band diode-laser radiation instead of sunlight should eliminate the disadvantage of lower absorption efficiency at cryogenic temperatures while the advantages (gain, thermal properties) should remain.

Therefore, the goal of this paper is to compare efficiences and thermal effects of cw side-pumped Nd:YAG rods for temperatures between 80 K and 380 K in order to find out whether cryogenic operation of diode-laser-pumped YAG lasers is advantageous.

1 Experimental

The Nd:YAG laser rod (diameter: 3 mm length: 35 mm in the laser measurements and 3 mm × 25 mm in the thermal measurements) and the diode-laser arrays are in a vacuum housing. The rod is attached to a water or liquid-nitrogen-cooled copper finger. Additional heating allows to set the temperature between 80 K and 380 K. Opposite the copper finger two Siemens 10 W linear diode-laser arrays are mounted on a thermo-electric cooler close to the YAG rod.

The laser experiments are carried out with a 20 cm long planoconcave resonator. The high reflector has a radius of curvature of 0.5 m. For outcoupling four different flat mirrors with transmissions between 0.3% and 8% are used. For each datapoint (diode current, rod temperature) the temperatures of the diode-laser arrays, the resonator and eventually the position of the arrays have to be optimized! Unfortunately, there is not much time to do this, because at low temperatures some outgasing of the electrical wiring and condensation on the endfaces of the rod occurs which degrades the laser performance within an hour. Therefore, the experimental error is of the order of ±10% to ±20%.

The thermal effects are measured with two different setups:

(i) A collimated HeNe-laser beam is passed through the laser rod and the deflection and focussing is measured with a CCD camera.

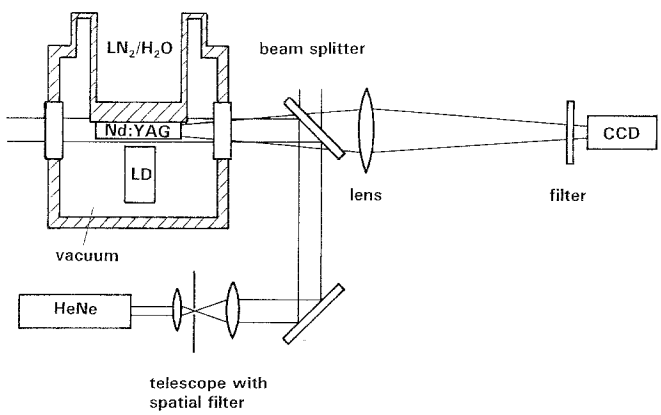

Fig. 1. Interferometric setup to measure the thermal effects in the Nd:YAG rod pumped by a Laser-Diode array (LD)

(ii) A collimated and expanded HeNe-laser beam is reflected from both ends of the YAG rod. Via a beam splitter and a lens the interference pattern is imaged onto the CCD chip (Fig. 1). This method was used for example by Veduta et al. [2] to measure thermal effects in flash-lamp-pumped ruby rods.

2 Results

2.1 Power Measurements

The Nd:YAG laser power versus pump power is measured for temperatures of 85, 135, 312, and 380 K and 4 different output couplers with transmissions of 0.35, 2.3, 5.1, and 8%. As an example the results obtained with the 2.3% output coupler are shown in Fig. 2. The temperature dependence of slope efficiency, extrapolated and real threshold are plotted in Figs. 3–5.

The slope efficiency of the 0.35% transmission laser is almost temperature independent (with a weak maximum around 250 K) while for higher output coupling (2.3%–8%) the slope efficiency increases with decreasing temperature by a factor of 2.5–3 between 380 K and 135 K. This behavior can be explained by two contrary effects occuring when cooling the crystal. The smaller absorption linewidths decrease the absorption efficiency, while the increasing peak emission cross section increases the gain and hence allows to extract laser power from a larger pump volume (especially for high transmission "losses").

Both the real and the extrapolated threshold decrease upon cooling, the extrapolated threshold by a factor of 2 to 3 from 380 K to below 100 K, the real threshold by a factor of 3 to 8 from 380 K to 85 K and by a factor of 2.5 to 4 between room temperature and 85 K. This is due to the narrowing of the emission lines. For example, the linewidth of the $R_1 \rightarrow Y_1$ transition decreases from 4 cm^{-1} (300 K) to $\sim 0.7\ cm^{-1}$ (< 50 K) [3]. The reduction factor of 6 gives only an indication about the increase in gain. This is because above 229 K Nd:YAG lases on the $R_2 \rightarrow Y_3$ transition (1064 nm) and only below 229 K on the $R_1 \rightarrow Y_1$ transition (1061 nm) [4]. In addition, one has to take into account the temperature dependence of the thermal population of the R_1 and R_2 levels.

The difference in real and extrapolated threshold reflects different laser mode volumes. Close to threshold only a small volume with low threshold (and low slope efficiency) contributes to lasing, while far above threshold a volume with higher threshold is added, increasing the slope efficiency.

The resonator losses can be determined

(1) by plotting threshold powers versus $(-\ln R)$, R being the reflectivity of the output coupler, and extrapolating to zero threshold (Findlay-Clay method) or
(2) from the slope efficiency η which is a product of the outcoupling efficiency $\eta_{oc} = T/(T+\varepsilon)$ and the excitation efficiency η_{exc} including all other efficiencies.

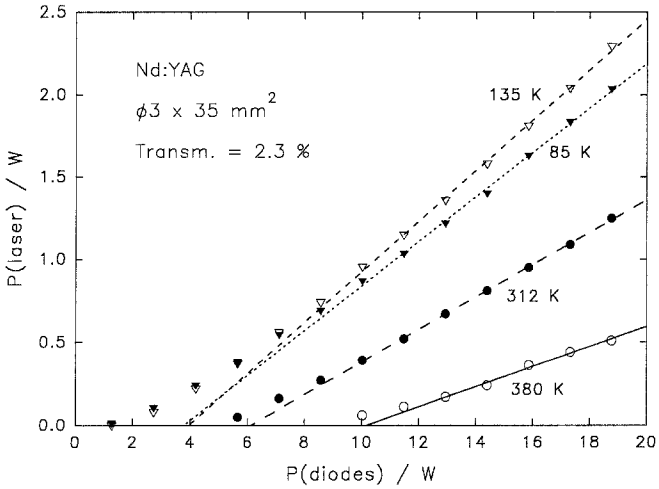

Fig. 2. Output power of the Nd:YAG laser vs the optical power of the diode-laser arrays for temperatures of 85, 135, 312, and 380 K and an output coupler transmission of 2.3%. For each data point the diode temperatures and the mirror alignment are optimized

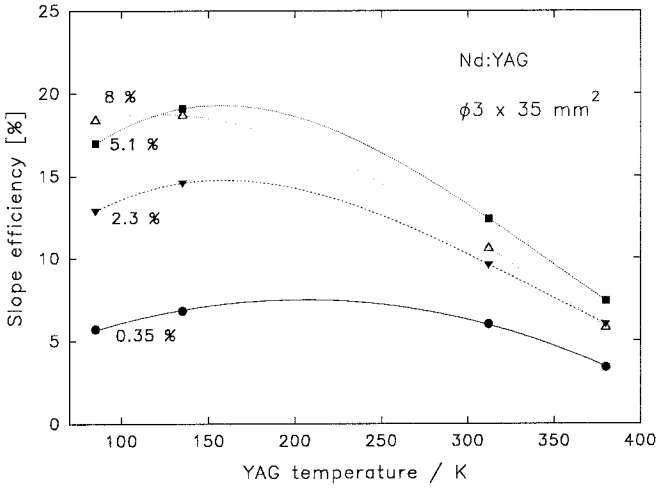

Fig. 3. Slope efficiency vs Nd:YAG temperature for output-coupler transmissions of 0.35, 2.3, 5.1, and 8%

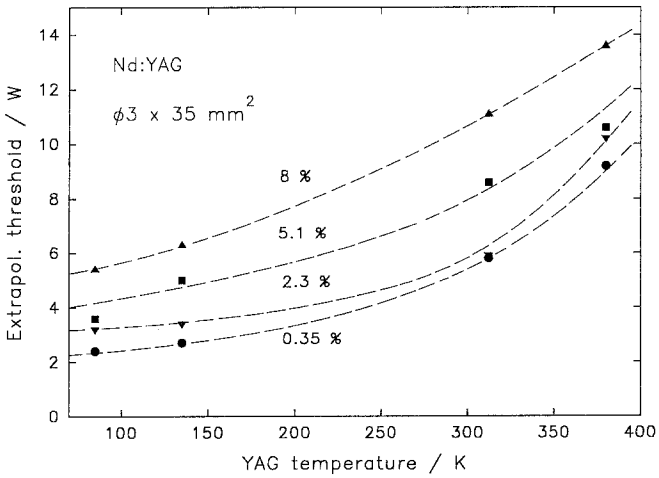

Fig. 4. Extrapolated threshold vs Nd:YAG temperature for output-coupler transmissions of 0.35, 2.3, 5.1, and 8%

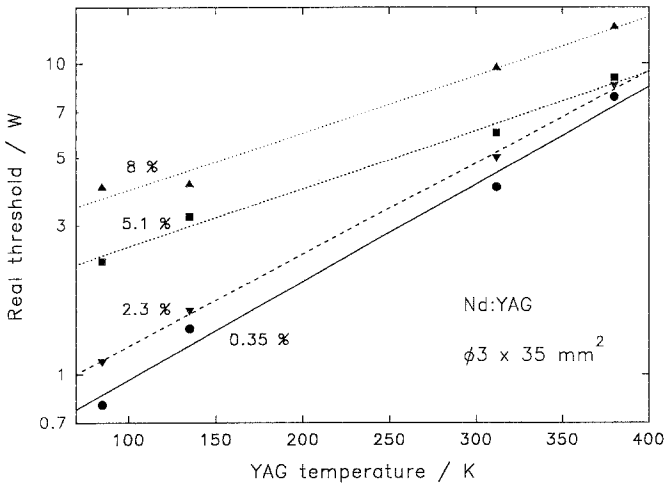

Fig. 5. Real threshold vs Nd:YAG temperature for output-coupler transmissions of 0.35, 2.3, 5.1, and 8% in logarithmic scale

Table 1. Internal losses determined with the method of Findlay-Clay and from the slope efficiency data

Method	Transm. [%]	Internal losses ε			
		85 K [%]	135 K [%]	312 K [%]	380 K [%]
1	–	1.0	3.1	5.1	11.6
2	0.35	1.8	1.5	1.7	3.3
	2.2	3.9	3.1	6.1	11.1
	5.1	5.2	4.2	9.3	19
	8.0	7.2	7.0	18	40

Table 2. Physical constants used for the calculations [5, 6]

	100 K	200 K	300 K	Units
Heat conductivity κ	0.58	0.21	0.13	$Wcm^{-1}K^{-1}$
Expansion coefficient α	4.25	5.8	7.5	$10^{-6}K^{-1}$
dn/dT	3.1	5.7	8.3	$10^{-6}K^{-1}$
Index of refraction n	–	–	1.82	

Assuming an excitation efficiency of 35% gives the best agreement for the internal losses ε calculated with both methods except for the figures for high transmissions and temperatures which seem to be systematically too high (Table 1). An explanation for this deviation could be that under these conditions the laser is working relatively close to threshold so that modes with lower threshold, but also poorer overlap between pump and laser-mode volume, i.e., lower excitation efficiency, oscillate. Discarding for this reason the numbers for high transmission and temperature internal losses of about 3% at 85 K and 135 K, 5% at 312 K, and maybe 10% at 380 K seem to be realistic.

The excitation efficiency of 35% is also confirmed by another observation. Switching on the laser pumped with 2.7 times the threshold pump power (at 100 K) reduces the spontaneous emission by 20% instead of 60% that would be expected for an excitation efficiency of 100%. This means that the actual excitation efficiency is about one third, provided the laser is operated a factor 2.7 above threshold.

2.2 Thermal Effects

The physical constants (Table 2) give already a first indication of the strong temperature dependence of the thermal effects. The heat conductivity κ increases by a factor of 4.5 from 300 K to 100 K and, at the same time, the thermal expansion and dn/dT decrease by a factor of 1.7 and 2.7, respectively. The experiments described in Sect. 2.1 give a further indication. For each diode current, i.e., pump power, the resonator has to be readjusted at or above room temperature while below 100 K there is no need at all for any resonator adjustments.

2.2.1 Beam Deflection Measurements. For rod temperatures between 80 K and 350 K the deflection of a collimated HeNe beam when passing through the rod are measured in several distances from the rod with a CCD camera. As expected, the deflection increases linear with pump power, at 320 K with 0.2 mrad/W of pump power. The beam deflection at fixed pump power, e.g., 2 × 9 W, versus rod temperature is also approximately a straight line with 1.45 mrad/100 K starting at 80 K (Fig. 6).

For a quantitative analysis the temperature gradient within the laser rod has to be estimated. The pumped region is assumed to be a slab of h = 3 mm, w = 1.2 mm, and l = 20 mm. Having an optical power of the diodes of 18 W, 15 W may be absorbed in the rod and one third of the 15 W, i.e., 5 W, may be transfered into heat (P_h). This gives a heat power density $q_h = P_h/V_{pump}$ of about

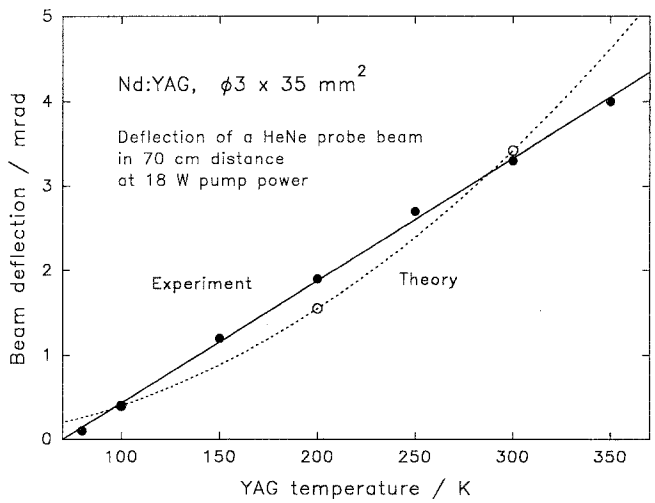

Fig. 6. Deflection of the HeNe probe beam in a distance of 70 cm at an optical power of the diode-laser arrays of 18 W. ●: experimental data, ○: data calculated with (5) and the constants of Table 2

70 W/cm^3 and a temperature difference

$$\Delta T = (h^2/2\kappa) q_h \quad (1)$$

of 24 K at 300 K, 15 K at 200 K, and 5 K at 100 K, respectively, for cooling on one side.

For the calculation of the beam deflection a linear temperature profile with a temperature difference ΔT across the rod is assumed. This gives
(1) an index gradient

$$n(x) = n_0(1-\xi x), \quad x = -h/2 \ldots +h/2 \quad (2)$$

with

$$\xi = \Delta n/2r = (dn/dT)(\Delta T/2r) \quad (3)$$

because of dn/dT and
(2) a wedge

$$\varphi_1 = -\varphi_2 = \Delta l/2h = (\alpha l/2h)\,\Delta T \quad (4)$$

because of the temperature dependent expansion coefficient $\alpha(T)$. φ_1 and φ_2 are the (small) angles between the endface normals and the rod axis. The change in the direction of the HeNe beam is then given by

$$\Delta r' \equiv r_{out}' - r_{in}' = (\varphi_2 - \varphi_1)(n_0 - 1)\, n_0 \xi l. \quad (5)$$

The results, calculated with the figures of Table 2 and the temperature difference ΔT from above, are also included in Fig. 6. They agree quite well with the experimental data, although the temperature difference ΔT and the linearization of the temperature gradient are somewhat arbitrary.

Several foci in the transmitted HeNe beam are also observed, the most pronounced in a distance of about 115 cm at room temperature. A calculation of the thermal lens of a slab with the dimension and heat load given above, gives a focal length of 90 cm in the x direction and 150 cm in the y direction [7]. At 100 K no signs of focussing within 1 m are observed, the calculation gives focal lengths of 10 m (x) and 22 m (y), respectively. Thus, also in this case theory and experiment are in reasonable agreement.

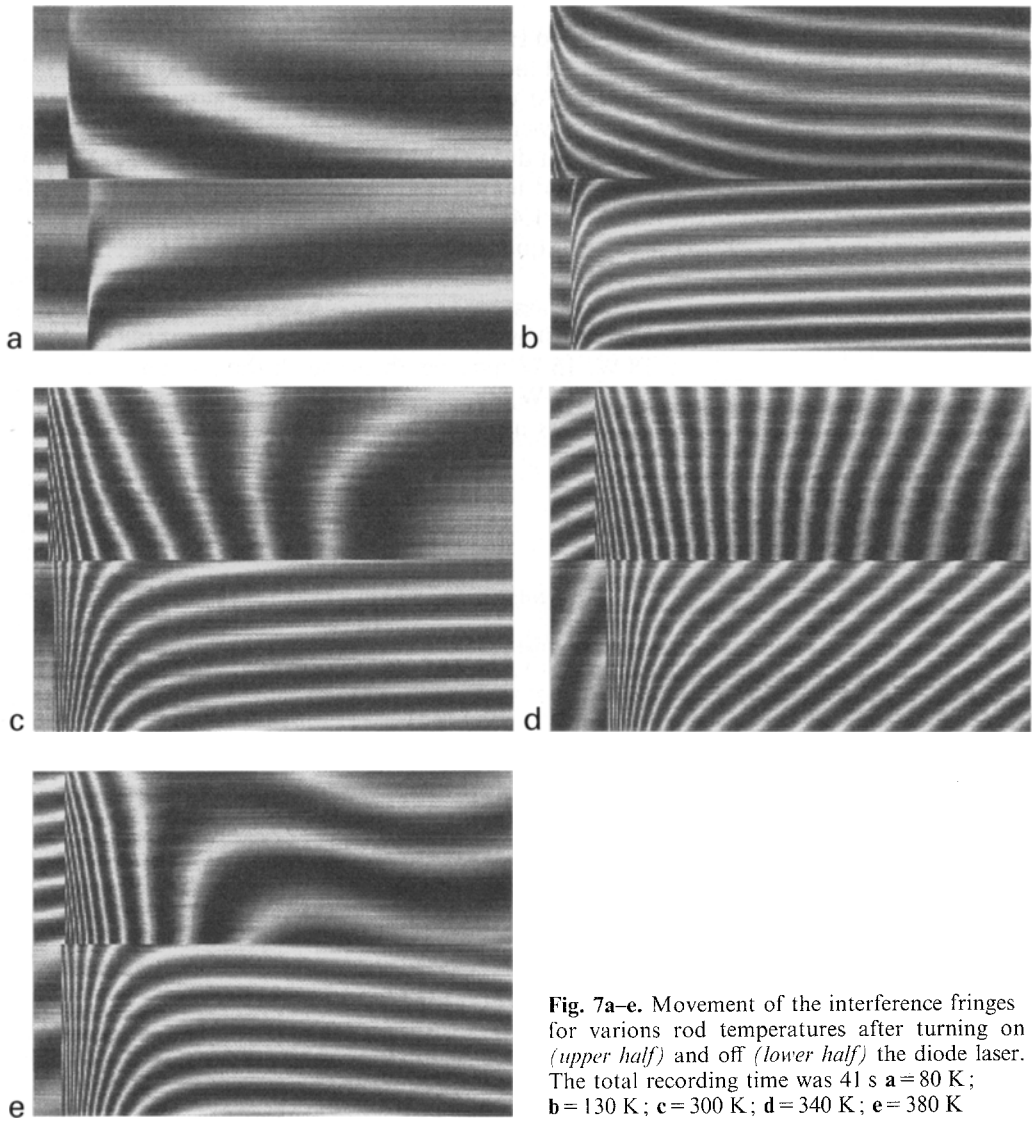

Fig. 7a–e. Movement of the interference fringes for varions rod temperatures after turning on *(upper half)* and off *(lower half)* the diode laser. The total recording time was 41 s **a** = 80 K; **b** = 130 K; **c** = 300 K; **d** = 340 K; **e** = 380 K

2.2.2 Interferometer Experiment. The laser rod is used as an interferometer (Fig. 1). The optical pump power is 4 W (one diode array with $I = 15$ A and an active length of $l = 10$ mm). The time dependent change of the approximately horizontal interference fringes when switching on and off the diode-laser array for various rod temperatures is shown in Fig. 7 a–e. For each picture thin vertical stripes of the interference pattern are cut at fixed time intervals and put together. Hence, the left-hand side of the upper half and the right-hand side of the lower half show the unpumped case, i.e., the wedge caused by the polishing of the rod. Inbetween is the transition zone of turning on (upper half) and turning off (lower half), respectively.

The difference in optical path length between upper and lower edge of the rod caused by the asymmetric heating and cooling as calculated from the change in the number of interference fringes is plotted in Fig. 8. The relation between path difference and temperature is approximately linear with 8 nm/K. Again, the optical path difference is caused by the change in the index of refraction and the change in the expansion:

$$\Delta l_{opt} = (dl_{opt}/dT)\,\Delta T, \tag{6}$$

$$dl_{opt}/dT = (dn/dT)\,l + n\,dl/dT. \tag{7}$$

The results also shown in Fig. 8 agree with the experimental data within the experimental error of ±20%.

In order to check this calculation, without having to go back to the relatively arbitrary ΔT that can only be estimated from the absorbed pump power and the geometry, another experiment is made where the whole laser rod is cooled from 300 K to 80 K and then heated up again. The temperature dependent pattern of interference fringes is recorded and the change of the number of fringes – or converted, $dl_{opt}(T)/dT$ – with temperature for several temperatures is calculated. Both the measured and calculated data are shown in Fig. 9. Again, they agree within the experimental error which means that the temperature differences ΔT that have been used in the analysis above are quite good.

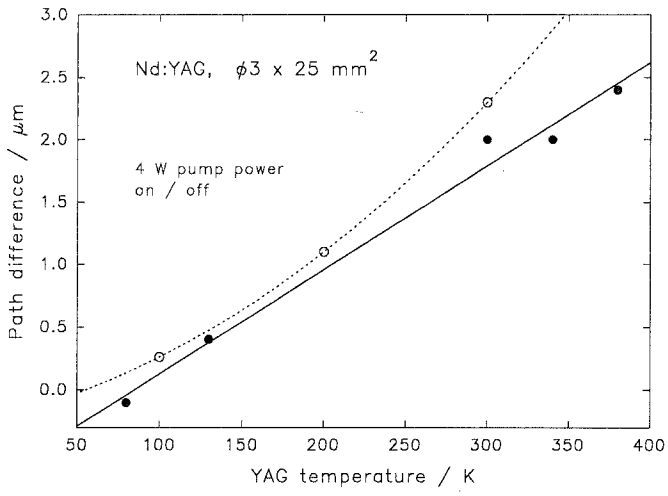

Fig. 8. Optical path difference in the vertical plane. ●: calculated from the increase/decrease of the number of interference fringes after turning on/off the 4 W diode-laser array; ○: calculated with (6) and the constants of Table 2

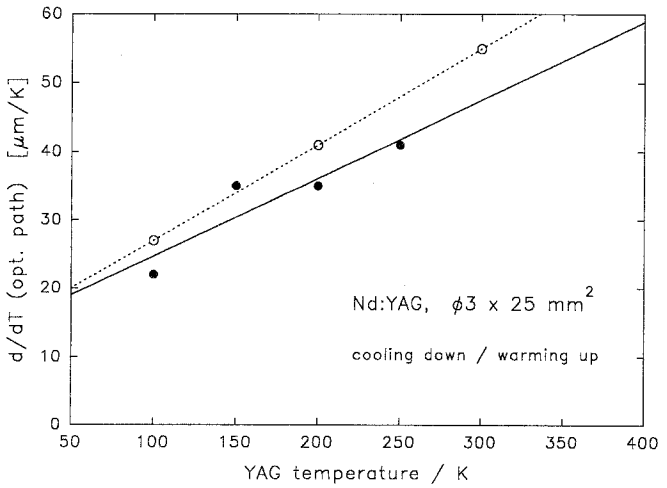

Fig. 9. Change of the optical length of the rod with temperature (dl_{opt}/dT) as a function of temperature. ●: measurement; ○: calculated with (7)

3 Discussion

Cooling to temperatures between 100 K and 150 K gives the maximum benefit for the Nd:YAG laser. It reduces the threshold considerably and increases the slope efficiency depending on the transmission of the output coupler. This results in an increase of the laser efficiency by a factor of 1.5–3. The maximum power with optimized output coupler is 2.5 W at 100 K and 1.3 W at 312 K. Of course, this depends strongly on the design of the laser, especially on the ratio of pump power to pumped cross-section area.

To get an idea of how the temperature effects the efficiency of a more powerful system, the data of the laser with about 20 W pump power and 2% transmission operated at 135 K and 312 K are extrapolated to a 240 W laser assuming the following:

(i) The cross-sectional area A is three times as large; this corresponds to a rod diameter of about 5 mm.
(ii) The excitation efficiency η_{exc} is 50% instead of the 35% of the small laser because of the higher pump power available and the larger cross section. Both allow a better overlap of pump and laser mode volume.
(iii) The internal losses are 50% higher because of the larger rod and the increased thermal load.

Then the slope efficiency η and the laser threshold P_{th} are calculated using:

$$\eta = \eta_{exc}\,T/(T+\varepsilon), \tag{8}$$

$$P_{th} \propto A(T+\varepsilon). \tag{9}$$

The results are given in Table 3. For a cw side-pumped laser an increase in efficiency of the order of 20–30% can be expected when operating the laser at 135 K instead of room temperature. This, in itself, is no argument for

Table 3. Extrapolation to a 240 W pumped laser using the results of the small laser pumped with 18 W (sect. 2.1) and (8, 9)

Laser	Transm. [%]	Temp. [K]	ε [%]	A	$P_{\text{pump}}^{\text{opt}}$ [W]	η_{exc} [%]	η [%]	P_{th} [W]	P_{out} [W]	$\eta_{\text{tot}}^{\text{opt}}$ [%]
Small	2	300	5	A_1	20	35	10	6	1.4	7
	2	135	3	A_1	20	35	14	3.5	2.3	12
Big	10	300	7.5	$3A_1$	240	50	29	45	57	24
	20	300	7.5	$3A_1$	240	50	36	71	61	25
	10	135	4.5	$3A_1$	240	50	34	30	71	30
	20	135	4.5	$3A_1$	240	50	42	51	78	32

low-temperature operation since the cryogenic cooling probably needs an additional 50% of the electrical power.

Much more important are the improved thermal properties of the YAG. The formation of a wedge due to the one-sided pumping and cooling is at 100 K only one tenth of the room-temperature value. Calculations show that this is because of a reduced temperature gradient (one fifth) and a reduced dn/dT and dl/dT (one half), respectively. This means that for a given pump power the thermal effects, e.g., thermal lensing, are reduced by the same factor of ten. Therefore, the cryogenic laser may be operated either with the same beam quality at ten times the output power or at the same output power with improved beam quality and less sensitivity of the beam parameters to changes in the average output power. This is of great interest in laser machining where a modulation of the laser over a wide power range is needed without change in beam quality.

The cryogenic cooling seems to be even more advantageous with the recently rediscovered (diode-laser-pumped) Yb:YAG system [8]. For relatively high pump power densities (ca. 10 kW/cm^2 or 50 kW/cm^3) an increase in efficiency and output power of about 50% is possible when cooling the Yb:YAG to 200 K or below [9]. For lower pump-power densities the gain when cooling is even higher. In addition, because of the extremely high efficiency of the material (< 10% quantum defect, ca. 85% slope efficiency below 200 K) there is very little heat that has to be taken away. Taking only the quantum defect into account it is about one third of the heat of diode-laser-pumped Nd:YAG.

4 Summary

Dependent on the design of the diode-laser-pumped Nd:YAG laser the lasing threshold is reduced by a factor of 2 to 4 when cooling the laser rod from room temperature to about 100 K due to the increased small signal gain. At the same time the slope efficiency is constant or slightly increased despite the reduced absorption linewidth. For a laser that operates significantly above threshold an increase of the optical efficiency of 25–30% at a temperature of 135 K can be expected. Because of the additional cooling power needed the total balance for cryogenic operation is likely to be worse.

An important advantage of the low temperature operation is the vastly improved thermal behavior. For example, the wedge formation due to asymmetric cooling and pumping is reduced by approximately a factor of ten between 300 K and 100 K. This means, for similar pump power – and even more for similar laser power – the thermal effects, e.g., thermal lensing, are reduced to one tenth of the room-temperature figure.

This is of special interest for a diode-laser-pumped Yb:YAG laser. As a quasi-two or three-level system it requires high pump-power densities and, therefore, excellent thermal properties. In addition, because of the marked reduction in the threshold and moderate increase in the slope efficiency, a positive power balance for cryogenic operation can be expected.

Acknowledgments. The author wishes to thank J. Muckenschnabel for his help in designing the laser, A. Voß, Institut für Strahlwerkzeuge, Universität Stuttgart, Germany, for his support in the interferometric measurements and W. Wittwer for the critical reading of the manuscript. The work reported here was done within a joint project sponsored by the Bundesminister für Forschung und Technologie.

References

1. U. Brauch, J. Muckenschnabel, G.A. Thompson, H. Bernstein, A. Yogev, A. Reich, M. Oron: Opt. Eng. **31**, 1072 (1992)
2. A.P. Veduta, A.M. Leontovich, V.N. Smorchkov: Sov. Phys.-JETP **21**, 59 (1965)
3. T. Kushida: Phys. Rev. **185**, 500 (1969)
4. M. Birnbaum, C.F. Klein: J. Appl. Phys. **44**, 2928 (1973)
5. W. Koechner: *Solid-State Laser Engineering,* 3rd edn., Springer Ser. Opt. Sci., Vol. 1 (Springer, Berlin, Heidelberg 1992) p. 51
6. A.V. Mezenov, L.N. Soms, A.I. Stepanov: J. Sov. Laser Res. **8**, 427 (1987)
7. J.M. Eggleston, T.J. Kane, K. Kuhn, J. Unternahrer, R.L. Byer: IEEE J. QE-**20**, 289 (1984); [5], p. 423, with Eq. (7.62) replaced by $f_{x,y} = [(N - S_{1,2})\, 2\, L]^{-1}$
8. P. Lacovara, H.K. Choi, C.A. Wang, R.L. Aggarwal, T.Y. Fan: Opt. Lett. **16**, 1089 (1991)
9. A. Giesen, H. Hügel, A. Voß, K. Wittig, H. Opower, U. Brauch: Appl. Phys. B (in press)